Al-Muthanna J. For Agric Sci Print ISSN: 2226-4086 Online ISSN:2575149
Vol. 12 , Issue 2. 2025

https://muthjas.mu.edu.iq/ http://doi.org/10.52113/mjas04/12.2/7

Performance Analysis of Hybrid Indirect Solar Dryer Featuring Multiple Absorber Plate Configurations

Abdulhadi Salahaldeen Abd[1] **Dr. Laith A. Zeinaldeen**[1]

Researcher **Assistant Professor**

[1]Department of Agricultural Machines and Equipment, College of Agricultural Engineering Sciences, University of Baghdad

E- mail : abd.abd2303m@coagri.uobaghdad.edu.iq E- mail : laith.a@coagri.uobaghdad.edu.iq

Abstract

A hybrid indirect solar dryer was locally assembled and fabricated in Baghdad, Iraq. The investigation focused on three factors. The first factor was the shape of the absorber plates with three levels: a flat plate, a vertically corrugated plate, and a perforated, horizontally corrugated plate. The second factor was the type of plate coating. Two types of matte black paint were used: smooth and rough paint. The third factor was the airflow rate. Three levels of air circulation within the dryer were examined: natural convection, single fan, and three fans.

The performance of the drying system was primarily evaluated based on the change in moisture content in onion slices. Accordingly, the interactions between these three factors were studied. The results indicated that the moisture content is affected by the temperature and the amount of air entering the dryer. The fastest reduction in moisture content (shortest drying time) was recorded when using three fans with a rough coating and a vertically corrugated plate (F2P2S2), reaching (125 minutes). Furthermore, the highest extracted energy of (2221.4 J/s) was obtained with natural convection with a rough coating and a vertically corrugated plate (F0P2S2). Additionally, the highest amount of quercetin was obtained when using three fans with a rough coating and a horizontally corrugated and perforated plate (F2P2S3), reaching (78.91 mg/100g).

Keywords: Hybrid indirect solar dryer, Absorber plate configuration, Airflow rate, Extracted energy, Moisture content.

Introduction

Food security and the imperative to adopt sustainable agricultural practices represent two critical global challenges in the current context. The significant spoilage of agricultural products in the post-harvest stage, a direct result of their high moisture content, is one of the primary causes exacerbating these challenges. Estimates indicate that losses in fruits and vegetables, particularly in developing countries, can reach 50% or more in some regions. These substantial losses are fundamentally attributed to the lack of appropriate post-harvest drying and storage technologies, according to the Food and Agriculture Organization (FAO, 1989). In the context of food security challenges, solar drying emerges as a practical and effective solution to address the significant spoilage of agricultural products. Despite the efficacy of conventional preservation methods, they often lack environmental sustainability due to their high energy consumption. Drying, as an ancient preservation technique, offers a viable solution, especially when integrated with renewable energy sources like solar power. Solar drying provides an environmentally friendly and economical alternative to fossil-fuel-dependent drying methods (Khayum et al., 2021), directly reducing greenhouse gas emissions and enhancing efforts to minimize post-harvest losses. The process of moisture removal (drying) occurs through two simultaneous mechanisms: heat transfer and mass transfer, and proceeds in two main stages (Ertekin & Yaldiz, 2004): In the first stage, moisture evaporates from the product surface at a constant rate. In the second stage, evaporation continues but at a falling rate, where the rate of product weight loss gradually decreases. Solar drying can be applied to all types of vegetables, fruits, grains, and herbs to produce products with better nutritional quality compared to those dried via other conventional drying operations (Kumar & Singh, 2020). The moisture content of fresh fruit varies widely, typically ranging between 20% and 90% (Ndukwu et al., 2020). It is worth noting that the required dryness levels for achieving safe and prolonged storage differ depending on the type of food and product. Solar drying stands out as one of the most important drying methods compared to other traditional styles, offering a range of operational, quality, and environmental advantages (Bahammou et al., 2019): It has lower operating costs, is a non-polluting process, reduces undesirable physical and chemical reactions, improves the quality of dried products, its temperature can be controlled, and it can be used for both direct and indirect heating. Open sun drying is the most widely used method for preserving agricultural products in most developing countries. However, conducting this process under hostile climatic conditions leads to severe losses in the quantity and quality of the final product (Pangavhane et al., 2002). These losses are

mainly attributed to contamination by dirt and dust, as well as infestation by insects, rodents, and animals. Therefore, the introduction of closed solar dryers in developing countries represents a strategic solution that significantly contributes to reducing crop losses and improving the quality of the dried product, compared to traditional drying methods such as direct sun drying or shade drying (Yaldiz et al., 2001). Solar dryers can be classified based on their airflow generation mechanism into natural convection (passive mode) and forced convection (active mode) solar dryers (Janjai & Bala, 2012). In natural convection solar dryers, airflow is generated automatically through the principle of buoyancy, where warmer, less dense air rises. In forced convection solar dryers, the necessary airflow is provided by a fan powered either by electricity, a solar unit or by fossil fuels. The indirect solar dryer is the oldest type of solar dryer, consisting of a separate solar collector characterized by a transparent top cover and a drying unit with an opaque top cover (Janjai & Bala, 2012). The main advantages of this design include its ability to preserve the quality of the dried product, the possibility of scientific control, and its ability to achieve a high drying rate (Belessiotis & Delyannis, 2011) (El-Sebaii & Shalaby, 2012) (Fudholi et al., 2010). Indirect solar dryers offer significant qualitative advantages, particularly concerning product quality. This is achieved by separating the drying chamber from the solar collector, which reduces direct exposure to solar radiation and prevents undesirable changes such as discoloration or scorching of the material being dried. This research focuses on enhancing the performance of a hybrid indirect solar dryer by evaluating the integration of various design techniques. This strategy aims to boost heat transfer efficiency, improve airflow management, and maximize energy utilization within the drying system. To achieve this, the effect of the interaction among three main factors on the overall system performance, which including moisture content, extracted energy, and quercetin concentration, was studied: 1-Absorber Plate Shape: Three shapes were tested: flat, vertically corrugated, and horizontally corrugated and perforated. 2-Number of Fans Used (Airflow Rate): Three ventilation levels were investigated: no fans (natural convection), single fan, and three fans. 3-Type of Coating Used on the Absorber Plate: Two finish levels were evaluated: smooth and rough. This study seeks to make an effective contribution to the post-harvest preservation of agricultural products through methods characterized by efficiency, sustainability, and reliability. Its ultimate goal is to support food security and promote environmentally sound agricultural practices. For this purpose, red onion was chosen as the product to be dried, using a locally fabricated hybrid indirect solar dryer. Onion is one of the most common vegetables globally, primarily used as a spice component in many countries. Onion contains a variety of chemical compounds

beneficial to health, such as fiber, vitamins, organic acids, as well as phenolic compounds and other antioxidants (Mitra et al., 2012). Onion possesses bioactive and curative properties related to its nutritional and health benefits, making it effective for use as a medicinal plant (Samtiya et al., 2021). Onion has a wide range of health effects, including antioxidant, anti-inflammatory, antidepressant, antibacterial, anti-proliferative, and wound-healing properties. Furthermore, it exhibits inhibitory activity against the enzymes trypsin and tyrosine and contains protective properties against cardiovascular diseases (Siddiq et al., 2013) (Dozio et al., 2015). Onion contains a variety of phenolic compounds that are of high nutritional and health importance. These compounds include Gallic acid, Ferulic acid, Protocatechuic acid, Quercetin, and Kaempferol (Cheng et al., 2013) (Pérez-Gregorio et al., 2010) (Singh et al., 2009). Both Gallic acid and Quercetin are considered vital compounds due to their multiple properties, including anti-allergic, antioxidant, anti-inflammatory, anti-hyperglycemic, anti-lipid peroxidation, and antimicrobial activities (Balasundram et al., 2006) (Cheng et al., 2013) (Mitra et al., 2012). These phenolic compounds are highly susceptible to temperature changes; therefore, maintaining their content requires the application of appropriate post-harvest treatments and effective storage methods. Drying is one of the most important of these treatments, where water content is removed by introducing heat (Djaeni et al., 2014). Harvested onion has a high moisture content, often exceeding 80% (Asiah et al., 2017), which can be reduced to 10% or less by drying, which in turn significantly increases the product's storage life.

Material and methods

This study encompassed a systematic performance evaluation of a locally manufactured and developed solar dryer. The design methodology commenced with the acquisition of climatic data pertinent to the study location in Baghdad, Iraq, followed by a thorough analysis of existing solar dryer designs to pinpoint their features and characteristics. The specific product selected for drying was determined by its suitability for the temperatures achievable by the solar dryer. To address the study's objectives, three identical solar dryers were constructed to accommodate the experimental factors: the first unit operated in a natural convection mode (passive mode), while the second and third units utilized a forced convection mode (active mode), achieved by incorporating one fan into the second dryer and three fans into the third.

The solar dryer is composed of two primary sections: a solar collector and a drying chamber. The entire dryer was coated with matte black paint to enhance solar energy absorption, a technique validated in prior research (Mokhtarian et al., 2020).

The two main components of the solar dryer are:

1- Solar Collector: This component is responsible for converting incident solar radiation into the thermal energy required for the drying process. The outer structure of the dryer was assembled using a combination of steel and wood. Steel with a thickness of (2 mm) was used for the main framework and the legs, while the structure and the base of the collector were made from plywood with a thickness of (1.75 cm). Wood was selected for its advantageous properties, including effective thermal insulation, lower thermal conductivity compared to metals, cost-effectiveness, lightweight nature, and being a non-carcinogenic and environmentally friendly material. The collector was built with dimensions of (2 m length), (0.75 m width), and (0.16 m height) (as illustrated in Figure 1). Inside, carbon steel absorber plates were installed in three distinct geometries: flat, vertically corrugated, and horizontally corrugated and perforated. These plates were subsequently treated with two variations of matte black paint (smooth and rough) to maximize solar radiation absorption. To protect the collector, it was covered with a transparent plastic sheet with a thickness of 4 mm, which is considered the best option according to reference (Bakari et al., 2014) due to its resistance to breakage, ease of handling, and maintenance. The collector was internally insulated using an Armaflex type foam insulator with a thickness of 0.01 meters. The purpose was to reduce thermal losses, insulate the collector from external environmental effects, and prevent any leakage, thereby helping to maintain the temperature and the efficiency of its transfer to the drying chamber. This insulator consists of a black, compressed foam layer, covered with an aluminum layer to enhance the thermal insulation efficiency and prevent heat leakage.

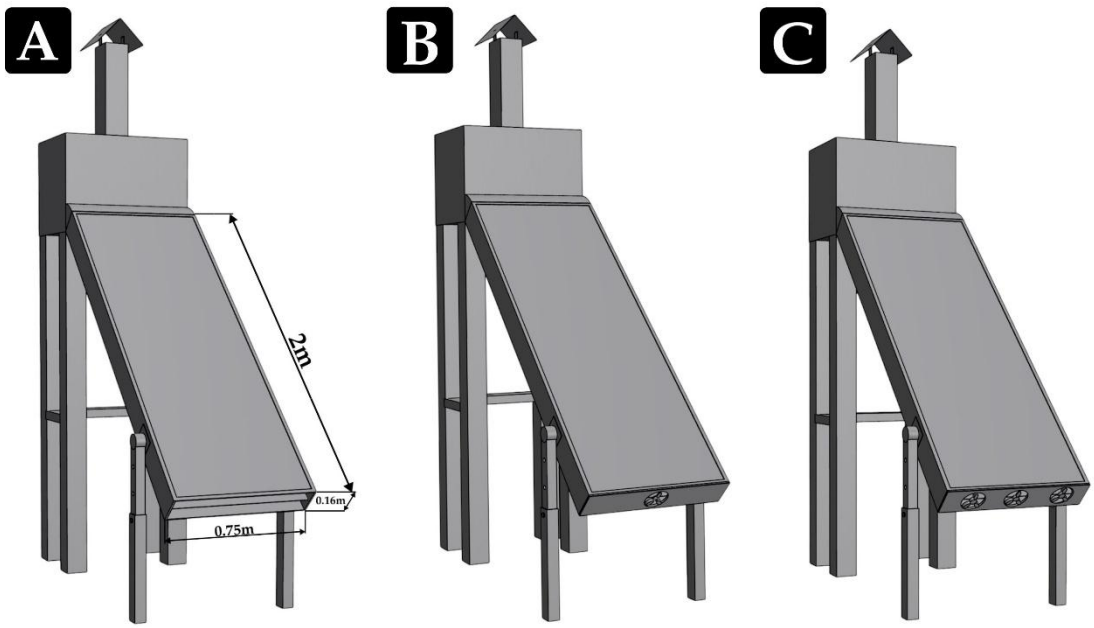

Figure 1. Front view of the solar dryer (three-dimensional shape) (A) Natural Convection (B) single Fan (C)Three Fans

To control the velocity and quantity of air flowing into the solar dryer, fans were installed in the second and third dryers. Fans of model HA1225M12S-Z were used, with dimensions of 120×120×25 mm (length x width x depth). These fans operate on direct current (DC) at a voltage of 12 volts and a current of 0.45 amperes, and they are powered by the solar power system.

2- The Drying Chamber: Positioned as the upper section of the solar dryer, the drying chamber was specifically engineered to be adaptable for drying a wide variety of medicinal plants. The chamber utilized a laminated wooden frame with a thickness of 1.75 cm, achieving dimensions of 0.5 m (length) x 0.75 m (width) x 0.55 m (height) (as depicted in Figure 2). To mitigate thermal losses, the drying chamber was insulated internally using the same insulator used in the collector, an Armaflex type, with a thickness of 0.01 meters. This was done with the aim of reducing thermal losses and insulating the chamber from the effects of the external environment, thereby helping to maintain a stable temperature inside the drying chamber. The chamber houses two drying racks, positioned with a vertical separation of 0.15 m. These racks were designed to be easily detachable to simplify the procedures for product loading, cleaning, and maintenance. Each rack is built using a wooden frame fitted with a rust-resistant aluminum mesh, which permits the unimpeded airflow from the lower rack to the upper rack, and subsequently towards the wet air exhaust vent (chimney) for expulsion to the external environment. To monitor environmental conditions, 18 DHT22 temperature sensors were used, connected to six key locations: one sensor to measure the external temperature, two in the solar collector, two above each drying rack, and one at the wet air exhaust vent.

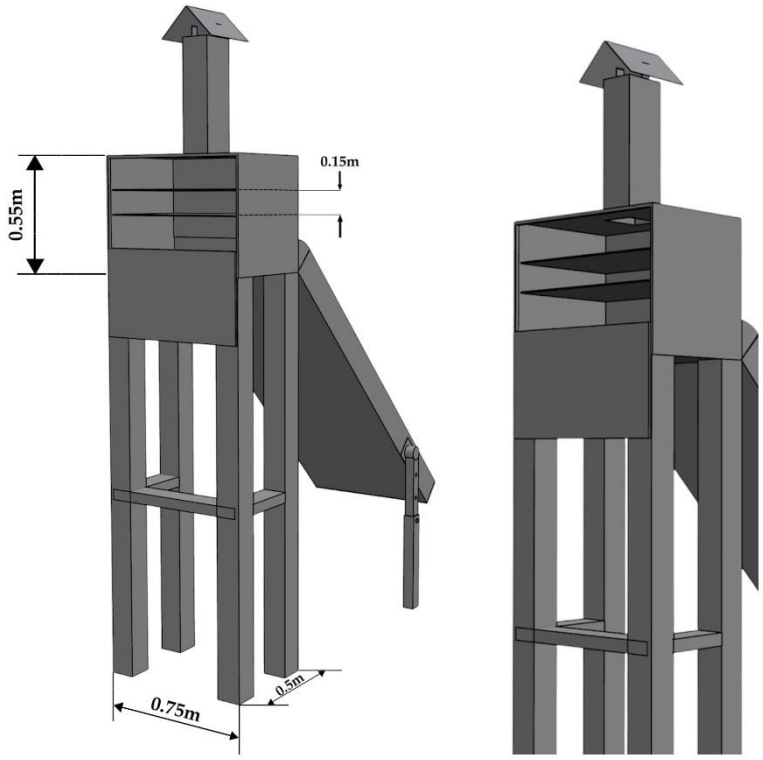

Figure 2. Back view of the solar dryer (three-dimensional shape)

Solar Power System: The solar power system consists of three main components: a solar panel, a voltage regulator, and a battery. The solar panel converts solar energy into electrical energy, with a capacity of 180 watts, a voltage of 23.4 volts, and a current of 9.71 amps. The voltage regulator (Solar Charge Controller) regulates the output voltage to 12 volts to suit the devices intended for operation. The battery is a TTNergy TT 100-12 Gel Deep Cycle model, with a voltage of 12 volts and a capacity of 100 amp-hours. It is used to store solar energy, and it is suitable for operating direct current (DC 12V) loads such as fans, pumps, and lighting, as its deep cycle design allows it to withstand repeated cycles of discharging and recharging (Shukir, 2021). This system is specifically used to power the fans, the Arduino electronic system, and the sensors.

The study encompassed three primary factors to evaluate the performance of the solar dryer. The first factor, the number of fans, was tested at three levels: no fans (F0), relying on natural convection; single fan (F1); and three fans (F2). The second factor included three different designs for the absorber plate shape: a flat plate (S1), a vertically stepped plate (S2), and a horizontally stepped and perforated plate (S3). The third factor, absorber plate paint type, involved two types of matte black paint: a smooth coating (P1) and a rough coating (P2).

Solar Collector Tilt

To enhance the performance of a solar collector, it is essential to correctly adjust its tilt angle. This angle allows for the absorption of the maximum amount of solar radiation by making the collector's surface as perpendicular as possible to the sunlight. Additionally, the tilt angle contributes to improving airflow within the system, based on the principle of natural convection, where warmer, less dense air rises.

$\beta=(\Phi-\square)$ .....(1)

$\square=23.45sin\{360/365\ (284+N)\}$ ..... (2)

Where: β is the angle of the solar collector with the horizon (º),

Φ is the degree of latitude (º),

δ is the angle of declination (º) with the direction south,

N is the number of the day (in January N = 1 and in December N = 365). (Cheng et al., 2013)

In accordance with equations (1) and (2), the solar collector was designed to operate at several different tilt angles, ranging from 30° to 60° relative to the horizontal. This flexible approach ensures the dryer operates with high efficiency throughout all seasons of the year, by achieving a position where the solar radiation is as perpendicular as possible to the collector's surface, thereby enhancing the energy absorption process.

The experimental methodology employed a Randomized Complete Block Design (RCBD) with three factors. The first and second factors were applied at three levels, while the third factor was applied at two levels. This was replicated three times for each condition, resulting in a total of 54 experimental units. The experiment commenced by sourcing red onion bulbs

from local markets during the 2025 season. These onions were cleaned, washed, and sliced. The initial moisture content of the slices was determined to be 87.5% on a wet basis, using the oven-drying method at 105°C until a constant weight was achieved, in accordance with (AOAC 1990) procedures. During the drying process, onion samples were weighed and placed on mobile, perforated aluminum mesh trays to facilitate airflow and simplify sample weighing and moisture content estimation. Temperatures inside and outside the dryer were recorded every 15 minutes using DHT22 sensors connected to an Arduino Mega 2560, which was selected for its multiple ports suitable for large projects. A Bluetooth device was connected to the Arduino to transmit data directly to a mobile phone. Additionally, solar radiation intensity was measured every 15 minutes using a Solar Power Meter (SM206-SOLAR), and the inlet air velocity was measured using an Anemometer (HP-866A), also every 15 minutes. These measurements were crucial for studying the efficiency of the solar collector, the drying rate, and the pressure differential.

Study Parameters

1- Energy Extracted

The amount of energy extracted from the solar collector, and can be calculated by the equations below (Schiavone et al., 2013)

$E = ma * (h\,f - h\,i)\,td$ .... (3)

$Q = ma * cp * (ti - to)td$ .... (4)

E, Q = total useful energy (kJ)

hf = final specific enthalpy (kJ/ kg)

hi = initial specific enthalpy (kJ/kg)

ma = mass airflow rate (kg/h)

cp = Air specific heat (kJ/kg.C)

ti, to =internal & external temperature (C)

2- Moisture Content

Moisture content is a scientific term used to measure the amount of water present in a specific material (such as food, soil, grains, wood, etc.). It is usually expressed as a percentage and can be represented in two ways: wet basis (wb) and dry basis (db) (Prakash & Kumar, 2017).

MCwb = (m_i-m_f)/m_i *100 …. (5)

MCwb: Moisture Content on a wet basis

mf = Dry mass (kg)

mi= Initial wet mass (kg)

3- Amount of Water to be Evaporated

The amount of water to be evaporated represents the quantity of water that must be removed from the product to reach the safe moisture ratio for storage. This quantity is calculated using the following equation (Prakash & Kumar, 2017)

Mw=Mp*((Mi-Mf))/((100-Mf)) …. (6)

MW= Mass of water to be evaporated (kg)

Mp: Mass of the material to be dried (kg)

Mi: Initial moisture content (%)

Mf: Final moisture content (%)

Extraction and Quantification of Quercetin Compounds

This section describes the procedures followed for the extraction of the quercetin compound from the dried plant samples and its quantitative evaluation using the High-Performance Liquid Chromatography (HPLC) technique.

Extraction of Compounds by Ultrasound

To prepare the sample, 20 grams of the finely ground dried plant were mixed with 100 mL of chloroform and placed on an electric shaker for 3 hours. This step aimed to remove fats/lipids from the sample. After removing the chloroform, the sample was dried at (50˚C) to ensure the complete elimination of solvent residues.

Following the drying process, 10 grams of the sample were taken for the extraction process using a solvent consisting of ethanol/water in a 70/30 volume/volume ratio. The extraction was performed using an Ultrasonic Bath at room temperature for one hour.

After filtration, 5 mL of the liquid extract was reserved for dosage determination. The solvent was removed from the extract using a rotary evaporator and the extract was dried at (40˚C) until a constant weight was reached. The dry extracts were stored in vials at (4˚C) to protect them from oxidation.

Quantitative Estimation of Phenolic Compounds

The quantitative estimation of the individual phenolic compounds was performed using a SYKAM reverse-phase HPLC system, equipped with a UV detector.

- Column Used: C18-OSD column with dimensions 25 cm x 4.6 mm.
- Column Temperature: Set at 30°C.
- Elution Method: Gradient elution was adopted using the following solvents:

1. Solvent (A): Methanol.
2. Solvent (B): 1% Formic acid, prepared in a 70 : 30 v/v ratio.

- Flow Rate: 1.0 mL/min.
- Injection Volume: 100 microliters of samples and standards were injected automatically using an autosampler.
- Spectrophotometric Measurement: Spectra were measured at a wavelength of 280 nm (Radovanovic et al., 2015).

The concentration of the substance in the sample is calculated by comparing the peak area resulting from the sample with the peak area resulting from a standard solution of known concentration.

$$C\ (sample) = C\ (st) \times \frac{A(sample)}{A(st)} \quad \ldots. (7)$$

C (sample)= Concentration of the sample (the compound to be measured).

C (st)= Concentration of the standard solution (reference material).

A (sample)= Peak area of the sample (from the analysis device, such as HPLC).

A (st)= Peak area of the standard solution.

The result obtained from this equation is then multiplied by the dilution factor and divided by the sample weight (in gm) or sample volume (in ml). All these calculations are automatically performed within the device, displaying the sample concentration directly.

Results and Discussion:

1- Quercetin Concentration

Figure (3) illustrates the effect of the number of fans (F), the type of coating (P), the shape of the absorber plate (S), and their interactions on the quercetin concentration (mg/ 100g) in the sample. The figure clearly indicates that the number of fans (F) has a significant effect on the quercetin concentration. The use of three fans (F2) recorded the highest quercetin concentration, reaching (70.94 mg/100g), whereas the use of natural convection (F0) and single fan (F1) recorded quercetin concentration of (63.65 mg/ 100g) and (50.26 mg/100g), respectively. This is attributed to the fact that the use of three fans contributes to an increase in airflow, thus accelerating the drying speed. This minimizes the duration the onion is exposed to heat, which helps in preserving the quercetin. The amount of quercetin is affected by an increase in temperature and the duration of heat exposure, higher temperatures and longer exposure lead to quercetin degradation and a reduction in its content in the sample. Figure (3) also reveals that the type of coating (P) has a significant effect on the rate of quercetin concentration. The use of rough paint (P2) recorded the highest quercetin concentration at (66.27 mg/ 100g), while the use of smooth paint (P1) recorded a lower content at (56.96 mg/100g). This is because the use of rough paint led to an increase in temperature within the permissible limit, which contributes to faster drying. Consequently, the exposure time of the onion slices to heat is reduced, thus preserving the quercetin concentration in the sample. As mentioned above, a reduced heat exposure time leads to a

higher rate of quercetin retention. Furthermore, Figure (3) indicates that the shape of the absorber plate (S) had a significant effect on the quercetin concentration rate. The vertically corrugated plate (S2) recorded the highest quercetin concentration at (65.63 mg/ 100g), while the flat plate (S1) and the horizontally corrugated and perforated plate (S3) recorded quercetin concentration of (61.39 mg/ 100g) and (57.82 mg/100g), respectively. The reason for this is that the use of the vertically corrugated plate (S2) yielded the highest drying rate and, thus, the shortest time, which aids in retaining the maximum amount of quercetin in the sample. As mentioned above, the lower the heat exposure time, the higher the retention rate of quercetin in the sample. Figure (3) also demonstrates a significant effect of the interaction between the number of fans and the type of coating used (F*P) on the quercetin concentration. The use of three fans (F2) with rough paint (P2) recorded the highest quercetin concentration at (75.36 mg/ 100g), while the lowest content was recorded when using natural convection (F0) with smooth paint (P1), at (47.12 mg/100g). Figure (3) further clarifies a significant effect of the interaction between the number of fans and the shape of the plate used (F*S) on the quercetin concentration. The use of three fans (F2) with the vertically corrugated plate (S2) recorded the highest quercetin concentration at (74.77 mg/ 100g), while the lowest content was recorded when using natural convection (F0) with the flat plate (51), at (46.41 mg/100g). Figure (3) also shows a significant effect of the interaction between the type of coating used and the shape of the plate (P*S) on the quercetin concentration. The use of rough paint (P2) with the vertically corrugated plate (S2) recorded the highest quercetin concentration at (70.2 mg/100g), whereas the lowest content was recorded when using smooth paint (P1) with the flat plate (S1), at (53.89 mg/100g).

Finally, Figure (3) indicates a significant effect of the triple interaction between the number of fans, the type of coating, and the shape of the absorber plate (F*P*S) on the quercetin concentration. The figure shows that the highest quercetin concentration was recorded with the interaction of (F2P2S3), reaching (78.91 mg/ 100g), and the lowest content was recorded with the interaction of (F0P1S1), at (44.34 mg/100g).

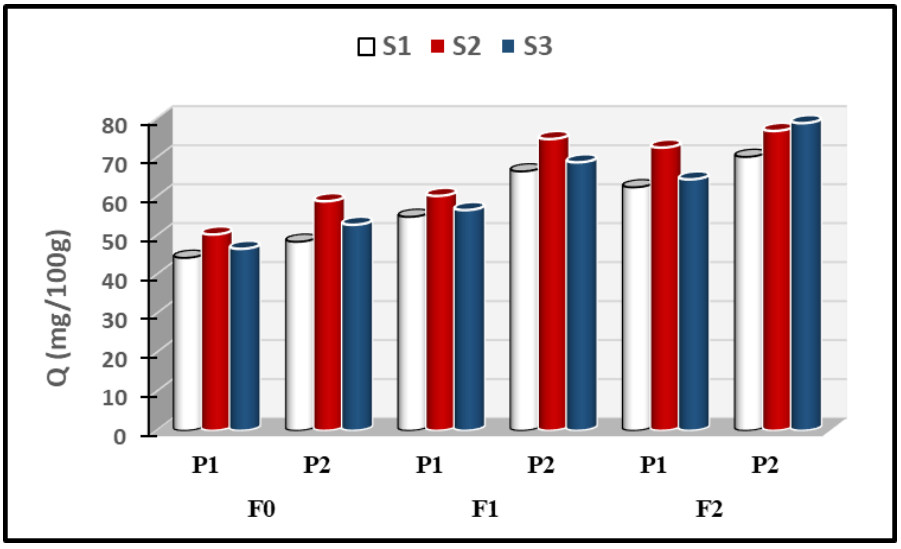

Figure 3. illustrates the effect of the number of fans, paint type, and absorber plate shape on the quercetin concentration (mg/ 100g).

2- Extracted Energy

The extracted energy in solar collectors is the thermal energy converted from solar radiation. It is calculated as the product of the air quantity (mass flow rate), the specific heat capacity of the air, and the difference between the temperatures inside and outside the solar collector. Figure (4) illustrates the effect of the number of fans (F), paint type (P), absorber plate shape (S), and their interactions on the rate of extracted energy (J/s) from the solar collector. The figure shows that the number of fans (F) has a significant effect on the extracted energy rate. The use of natural convection (F0) recorded the highest rate at (1781.6 J/s), while the use of single fan (F1) and three fans (F2) recorded extracted energy rates of (1640.2 J/s) and (703.5 J/s), respectively. This is because natural convection contributes to the calm (lower velocity compared to others) entry of a large quantity of air. The lower velocity allows for a longer heat exchange period between the incoming air and the absorber plate, which helps increase the temperature difference (ΔT) between the inside and outside of the dryer. Consequently, the extracted energy quantity increases, as it is directly proportional to the air quantity and the temperature difference between the inlet and outlet, as shown in Equation (3). This finding is consistent with (Balbine et al., 2015). From Figure (4), it is clear that the paint type (P) has no significant difference in the quantity of extracted energy. The use of smooth paint (P1) and rough paint (P2) showed extracted energy rates of (1404.3 J/s) and (1345.8 J/s), respectively. We also note from Figure (4) that the plate shape (S) has a significant effect on the extracted energy rate. The vertically corrugated plate (S2) recorded the highest rate of extracted energy at (1425.6 J/s), while the horizontally corrugated plate (S3) and the flat plate (S1) recorded extracted energy rates of (1327.2 J/s) and (1372.3 J/s), respectively. The reason for this is that the use of the vertically corrugated plate helps raise the surrounding air temperature more than the flat plate because its initial area before corrugation is larger. This increases the contact surface area between the air entering the drying chamber and the absorber plate, thereby increasing the temperature difference between the inlet and outlet. Furthermore, the vertically corrugated plate is superior to the horizontally corrugated plate in terms of the quantity of incoming air, as its vertical corrugations are parallel to the direction of the airflow, causing no obstruction, unlike in (S3). As we know, the air quantity and the temperature difference are directly proportional to the amount of extracted energy, which is why (S2) yielded the highest amount of extracted energy. Figure (4) also shows a significant effect of the interaction between the number of fans and the type of coating used (F*P) on the extracted energy rate. The use of natural convection (F0) with rough paint (P2) recorded the highest extracted energy rate at (1927.4 J/s), and the lowest rate was recorded when using one fan (F1) with smooth paint (P1), at (702.9 J/s). From Figure (4), a significant effect of the interaction between the number of fans and the shape of the plate used (F*S) on the extracted energy rate is evident. The use of natural convection (F0) with the vertically corrugated plate (S2) recorded the highest extracted energy rate at (1927.8 J/s), while the lowest rate was recorded when using single fan (F1) with the flat plate (S1), at (690.2 J/s). Figure (4) also illustrates a

significant effect of the interaction between the type of coating used and the shape of the plate (P*S) on the extracted energy rate. The use of rough paint (P2) with the vertically corrugated plate (S2) recorded the highest extracted energy rate at (1522.1 J/s), while the lowest rate was recorded when using rough paint (P2) with the flat plate (S1), at (1299.6 J/s). Finally, Figure (4) indicates a significant effect of the triple interaction between the number of fans, the paint type, and the absorber plate shape (F*P*S) on the extracted energy rate. The figure shows that the highest extracted energy rate was recorded with the interaction of (F0P2S2), reaching (2221.4 J/s), and the lowest rate was recorded with the interaction of (F1P1S1), at (670.5 J/s).

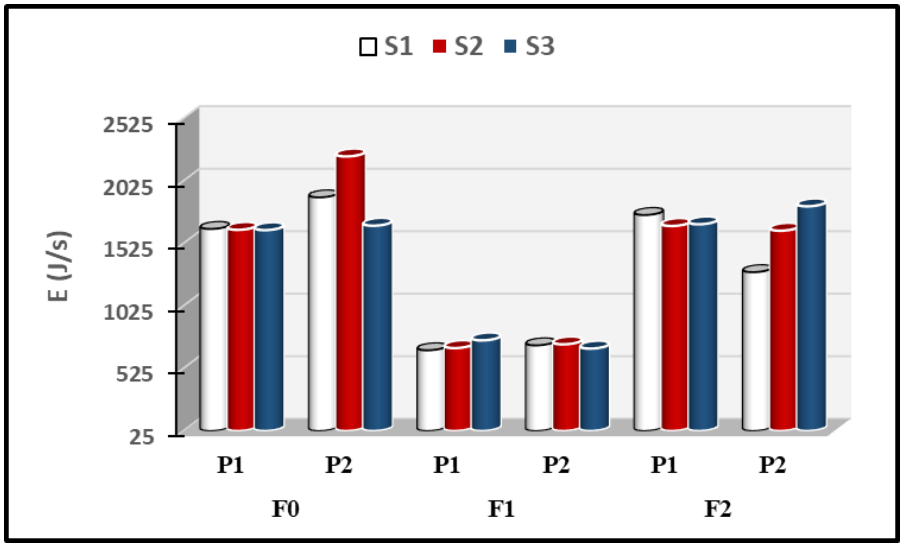

Figure 4. Effect of number of fans, type of coating and shape of absorbent plate on energy extracted (J/s)

3- Moisture Content

Moisture content refers to the actual quantity of water present within the product intended for drying. The fundamental goal of the drying process is to remove this amount of water to bring the product down to a specific, safe moisture ratio. This safe ratio is the operational criterion that determines the end of the drying process, as it is essential for ensuring product stability, maintaining its quality, and preventing the growth of microorganisms that cause spoilage during storage. Therefore, the operating mechanism aims to monitor the mass loss to reach this safe ratio, as detailed in the Materials and Methods section. The change in moisture content here is analyzed based on time, given that the final moisture content is constant. Figures (5) to (11) illustrate the effect of the number of fans (F), paint type (P), absorber plate shape (S), and their interactions on the moisture content over time. Figure (5) shows that the number of fans (F) has a significant effect on the moisture content. The use of three fans (F2) gave the fastest reduction in moisture level, reaching 140 minutes, while the use of natural convection (F0) and single fan (F1) recorded moisture level reductions of 150 minutes and 155 minutes, respectively. The reason for this is that the use of three fans resulted in the

highest airflow rate, which increased the rate at which evaporated moisture was expelled from the drying chamber, thereby achieving the shortest time.

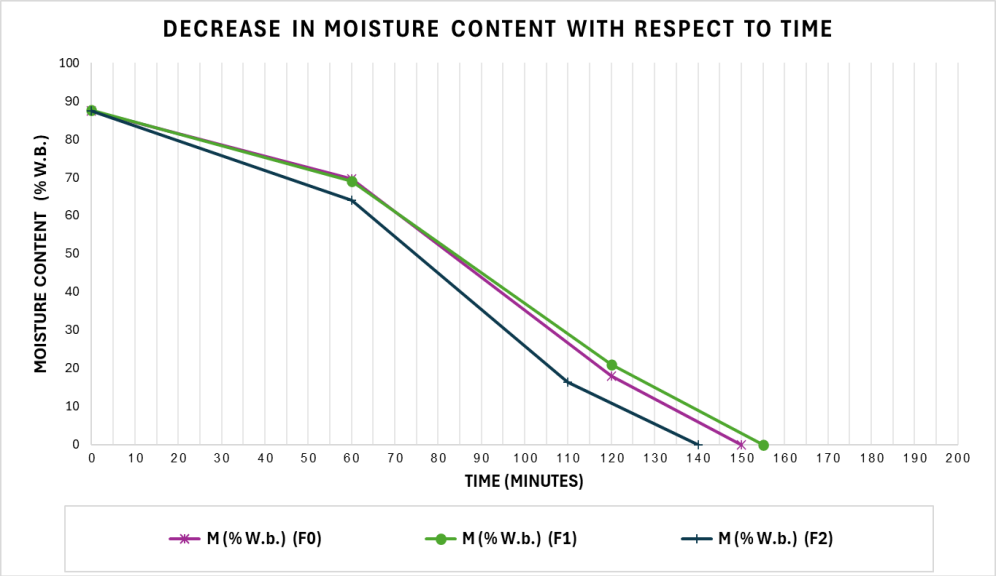

Figure 5. Effect of the number of fans on the rate of humidity reduction

Figure (6) indicates that the paint type (P) has a significant effect on the moisture content. The use of rough paint (P2) gave the fastest reduction in moisture level, reaching 140 minutes, while the use of smooth paint (P1) recorded a slower reduction in moisture level, reaching 155 minutes. The reason for this is that the use of a rough plate helps to increase heat absorption and reduces light reflection, because the rough surface scatters the incident light, thereby increasing the amount of absorbed energy. Roughness also contributes to an increase in the contact area between the hot air and the absorber plate. All these factors contribute to increasing the temperature of the absorber plate and, consequently, increasing the temperature of the air entering the drying chamber. This led to an increase in the amount of moisture evaporated from the product and thus reduced the time required for drying to reach the safe moisture ratio.

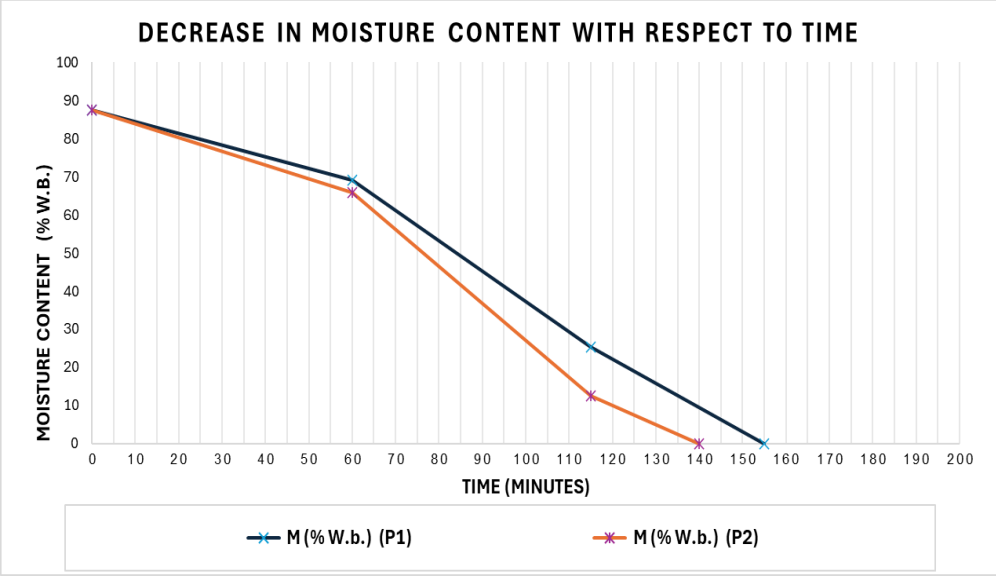

Figure 6. Effect of the type of paint used on the rate of moisture reduction

Figure (7) also shows that the shape of the absorber plate (S) had a significant effect on the moisture content. The horizontally corrugated and perforated plate (S3) recorded the fastest reduction in moisture level, reaching 145 minutes, while the flat plate (S1) and the vertically corrugated plate (S2) recorded moisture level reductions of 150 minutes and 155 minutes, respectively. The reason the horizontally corrugated and perforated plate achieved the fastest reduction in moisture level is due to its distinct design, which is horizontally stepped, counter to the direction of the air currents. This design works to scatter the air inside the solar collector and slow it down, which increases the duration of heat exchange between the plate and the air entering the drying chamber. This leads to an increase in the air temperature, which subsequently increases the amount of evaporated moisture and, in turn, reduces the time required for the drying process.

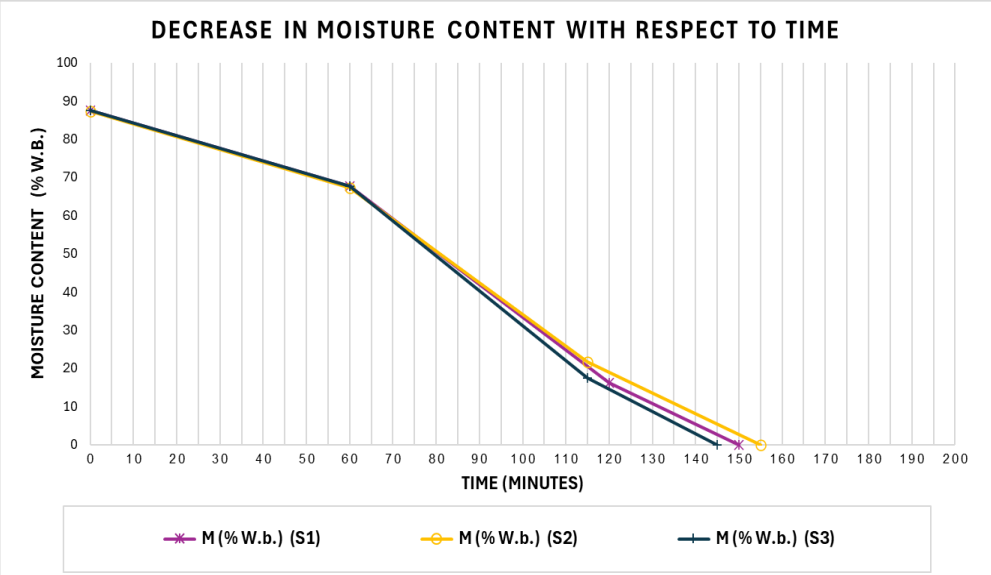

Figure 7. Effect of the type of absorbent plate used on the rate of moisture reduction

Figure (8) also reveals a significant effect of the interaction between the number of fans and the paint type used (F*P) on the moisture content. The use of three fans (F2) with rough paint (P2) recorded the fastest rate of moisture content reduction, reaching 135 minutes, whereas the slowest rate of moisture reduction was recorded when using single fan (F1) with smooth paint (P1), at 170 minutes.

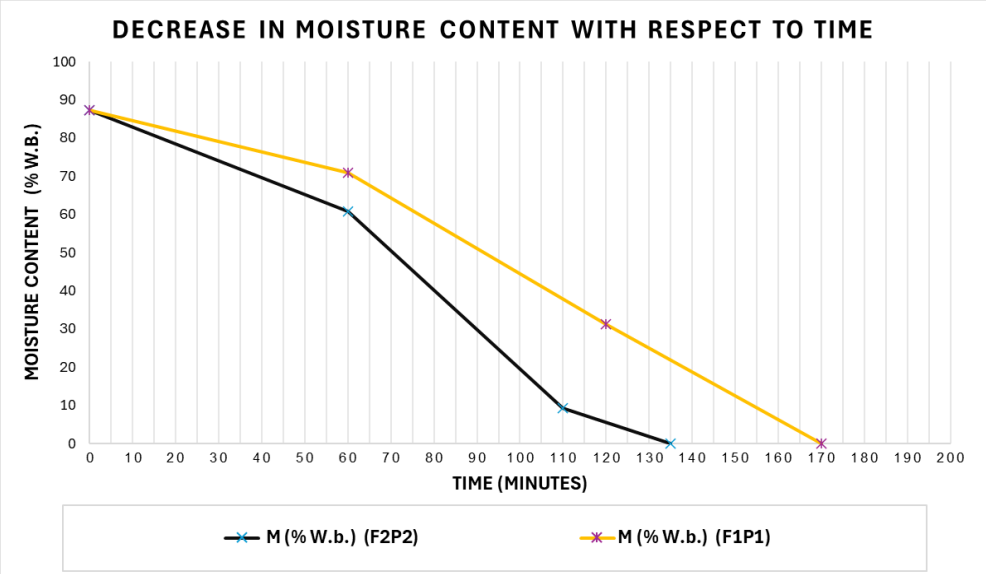

Figure 8. The effect of the dual interaction between the number of fans and the type of paint on the rate of moisture reduction

Figure (9) also demonstrates a significant effect of the interaction between the number of fans and the shape of the plate used (F*S) on the moisture content. The use of three fans (F2) with the horizontally corrugated and perforated plate (S3) recorded the fastest rate of moisture reduction, reaching 135 minutes, whereas the slowest rate of moisture reduction was recorded when using natural convection (F0) with the vertically corrugated plate (S2), at 165 minutes.

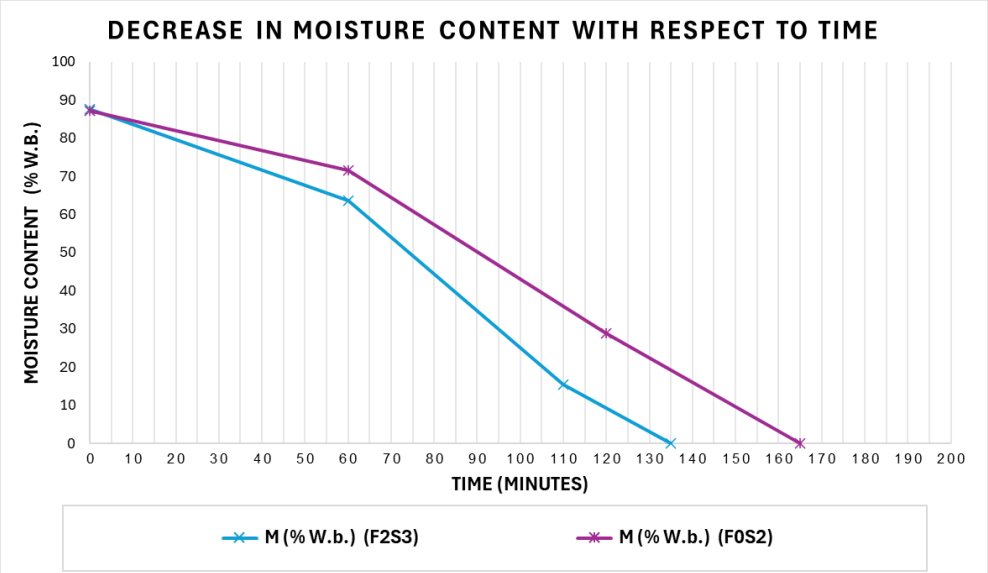

Figure 9. The effect of the dual interaction between the number of fans and the shape of the panel used on the rate of humidity reduction

Figure (10) also illustrates a significant effect of the interaction between the type of coating used and the shape of the plate (P*S) on the moisture content. The use of rough paint (P2) with the horizontally corrugated and perforated plate (S3) recorded the fastest rate of moisture reduction, reaching 140 minutes, whereas the slowest rate of moisture reduction was recorded when using smooth paint (P1) with the vertically corrugated plate (S2), at 160 minutes.

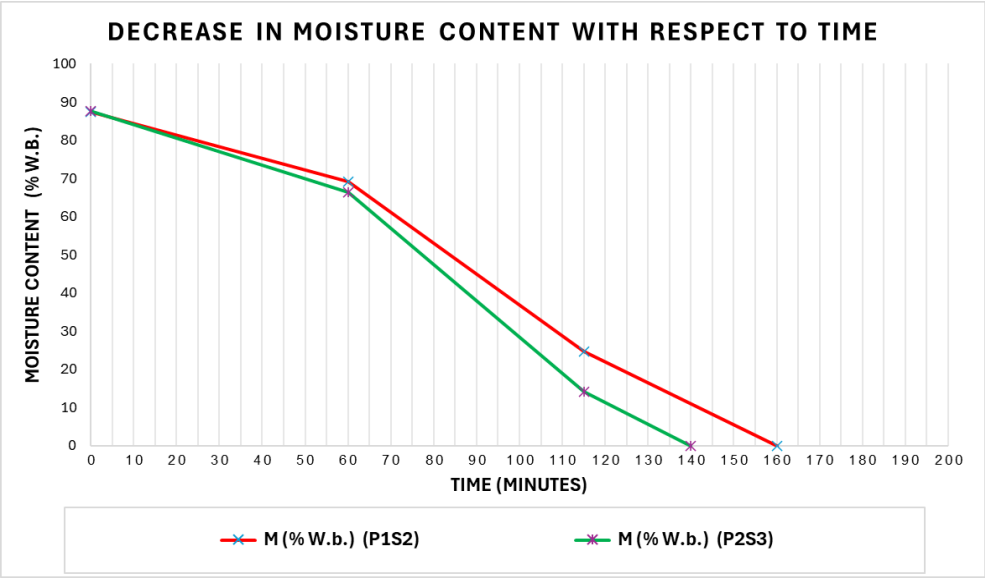

Figure (10) The effect of the dual interaction between the type of paint used and the shape of the board on the rate of moisture reduction

Figure (11) demonstrates a significant effect of the triple interaction between the number of fans, the type of coating, and the shape of the absorber plate (F*P*S) on the moisture content. The figure shows that the fastest rate of moisture reduction (shortest drying time) was recorded with the interaction of (F2P2S2) (three fans, rough paint, vertically corrugated plate), reaching 125 minutes, while the slowest rate of moisture reduction (longest drying time) was recorded with the interaction of (F1P1S3) (single fan, smooth paint, horizontally corrugated and perforated plate), at 185 minutes.

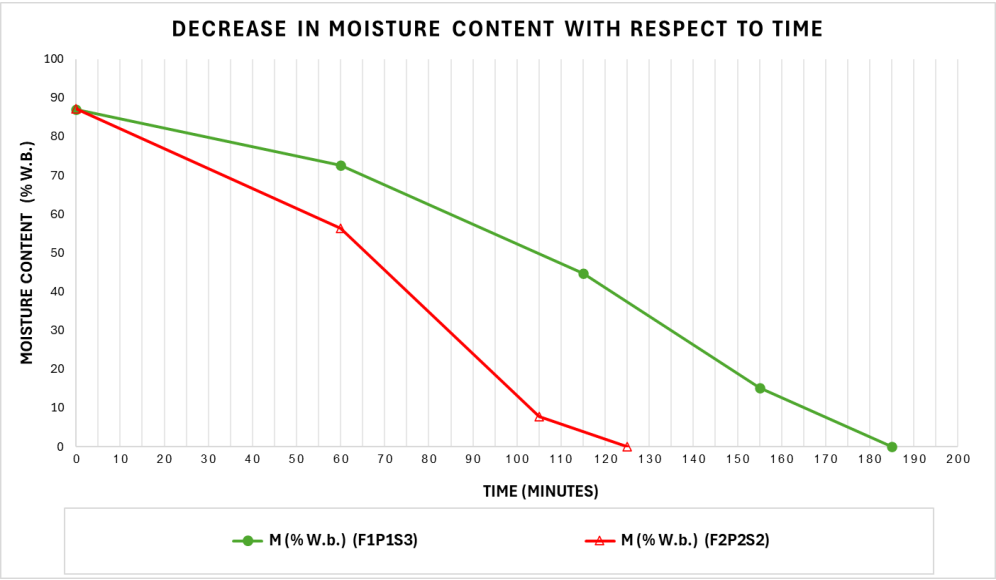

Figure 11. The effect of the number of fans, type of paint, and shape of the absorbent board on the rate of humidity reduction

Conclusions

1- The use of three fans (F2) increases the velocity and volume of the incoming air, leading to a faster reduction in moisture content.
2- The use of natural convection (F0) increases the temperature difference between the inside and outside, leading to the highest extracted energy.
3- The highest amount of quercetin was obtained with the triple interaction of the fans, rough paint, and the horizontally corrugated and perforated plate (F2P2S3).

References:

Asiah, N., Djaeni, M., & Hii, C. L. (2017). Moisture Transport Mechanism and Drying Kinetic of Fresh Harvested Red Onion Bulbs under Dehumidified Air. *International Journal of Food Engineering*, 13(9). https://doi.org/10.1515/ijfe-2016-0401

Bahammou, Y., Tagnamas, Z., Lamharrar, A., & Idlimam, A. (2019). Thin-layer solar drying characteristics of Moroccan horehound leaves (Marrubium vulgare L.) under natural and forced convection solar drying. *Solar Energy*, 188(May), 958–969. https://doi.org/10.1016/j.solener.2019.07.003

Bakari, R., Minja, R. J. A., & Njau, K. N. (2014). Effect of Glass Thickness on Performance of Flat Plate Solar Collectors for Fruits Drying. *Journal of Energy*, 2014(March), 1–8. https://doi.org/10.1155/2014/247287

Belessiotis, V., & Delyannis, E. (2011). Solar drying. *Solar Energy*, 85(8), 1665–1691. https://doi.org/10.1016/j.solener.2009.10.001

Bharadwaz, K., Barman, D., Bhowmik, D., & Ahmed, Z. (2017). Design, fabrication and performance evaluation of an indirect solar dryer for drying agricultural products. *International Research Journal of Engineering and Technology*, 4(7), 1684-1692.

Cheng, A., Chen, X., Jin, Q., Wang, W., Shi, J., & Liu, Y. (2013). Comparison of phenolic content and antioxidant capacity of red and yellow onions. *Czech Journal of Food Sciences*, 31(5), 501–508. https://doi.org/10.17221/566/2012-cjfs

Das, B., Mondol, J. D., Debnath, S., Pugsley, A., Smyth, M., & Zacharopoulos, A. (2020). Effect of the absorber surface roughness on the performance of a solar air collector: an experimental investigation. *Renewable Energy*, 152, 567-578.

Demissie, Y. A., Abreham, R. E., Wassie, H. M., & Getie, M. Z. (2024). Advancements in solar greenhouse dryers for crop drying. *Energy Reports*, 11, 5046-5058.

Djaeni, M., Anggoro, D., Santoso, G. W., Agustina Sari, D., Asiah, N., & Hii, C. L. (2014). Enhancing the food product drying with air dehumidified by zeolite. *Advance Journal of Food Science and Technology*, 6(7), 833–838. https://doi.org/10.19026/ajfst.6.120

Dozio, E., Barassi, A., Ravelli, A., Angeli, I., Lodi, F., Melzi d'Eril, G. V., & Corsi Romanelli, M. M. (2015). The "Breme" red onion: effects of home-storage methods on

quercetin and quercetin-glycoside contents. *Czech Journal of Food Sciences*, 33(5), 405-409.

El-Sebaey, M. S. (2024). Proposing novel approach for indirect solar dryer integrated with active-fan and passive-chimney: An experimental and analytical investigation. *Energy*, 304, 132215.

El-Sebaii, A. A., & Shalaby, S. M. (2012). Solar drying of agricultural products: *A review. Renewable and Sustainable Energy Reviews*, 16(1), 37–43. https://doi.org/10.1016/j.rser.2011.07.134

Ennissioui, J., & El Rhafiki, T. (2023). Experimental study of a natural convection indirect solar dryer. Heliyon, 9(11).

Ertekin, C., & Yaldiz, O. (2004). Drying of eggplant and selection of a suitable thin layer drying model. *Journal of Food Engineering*, 63(3), 349–359. https://doi.org/10.1016/j.jfoodeng.2003.08.007

Food and Agriculture Organization of the United Nations. (1989). Prevention of post-harvest food losses fruits, vegetables and root crops: A training manual. Rome, Italy: Author.

Goud, M., & Reddy, M. V. V. (2019). A novel indirect solar dryer with inlet fans powered by solar PV panels: Drying kinetics of Capsicum Annum and Abelmoschus esculentus with dryer performance. *Solar Energy*, 194, 871-885.

Janjai, S., & Bala, B. K. (2012). Solar Drying Technology. *Food Engineering Reviews*, 4(1), 16–54. https://doi.org/10.1007/s12393-011-9044-6

Jin, W., Mujumdar, A. S., Zhang, M., & Shi, W. (2018). Novel Drying Techniques for Spices and Herbs: a Review. *Food Engineering Reviews*, 10(1), 34–45. https://doi.org/10.1007/s12393-017-9165-7

Jindal, V. K., & Gunasekaran, S. (1982). Estimating Air Flow and Drying Rate Due to Natural Convection in Solar Rice Dryers. *In Renwable Energy Review Journal* (Vol. 4, Issue 2, pp. 1–9).

Khama, R., Aissani, F., & Alkama, R. (2016). Design and performance testing of an industrial-scale indirect solar dryer. *Journal of Engineering Science and Technology*, 11(9), 1263-1281.

Khayum, N., Anbarasu, S., & Murugan, S. (2021). Optimization of fuel injection parameters and compression ratio of a biogas fueled diesel engine using methyl esters of waste cooking oil as a pilot fuel. *Energy*, 221, 119865. https://doi.org/10.1016/j.energy.2021.119865

Kokate, Y. D., Baviskar, P. R., Baviskar, K. P., Deshmukh, P. S., Chaudhari, Y. R., & Amrutkar, K. P. (2023). Design, fabrication and performance analysis of indirect solar dryer. Materials Today: Proceedings, 77, 748-753.

Kong, D., Wang, Y., Li, M., & Liang, J. (2024). A comprehensive review of hybrid solar dryers integrated with auxiliary energy and units for agricultural products. *Energy*, 293, 130640.

Kumar, P., & Singh, D. (2020). Advanced technologies and performance investigations of solar dryers: A review. *Renewable Energy Focus* , 35, 148–158. https://doi.org/10.1016/j.ref.2020.10.003

Matouk, A. M., EL-Kholy, M. M., Tharwat, A., Elfar, S. E., & Shehata, E. A. (2021). Drying of Onion Slices Using Hybrid Solar Dryer. *Journal of Soil Sciences and Agricultural Engineering*, 12(7), 491-498.

Mitra, J., Shrivastava, S. L., & Rao, P. S. (2012). Onion dehydration: A review. *Journal of Food Science and Technology*, 49(3), 267–277. https://doi.org/10.1007/s13197-011-0369-1

Mohammed, S. A., Alawee, W. H., Chaichan, M. T., Abdul-Zahra, A. S., Fayad, M. A., & Aljuwaya, T. M. (2024). Optimized solar food dryer with varied air heater designs. *Case Studies in Thermal Engineering*, 53(October 2023), 103961. https://doi.org/10.1016/j.csite.2023.103961

Mokhtarian, M., Kalbasi-Ashtari, A., & Hamedi, H. (2020). Effects of shade and solar drying methods on physicochemical and sensory properties of Mentha piperita L. *Food and Health*, 3(3), 25–32.

Ndukwu, M. C., Simo-Tagne, M., & Bennamoun, L. (2020). Solar drying research of medicinal and aromatic plants: An African experience with assessment of the economic and environmental impact. *African Journal of Science, Technology, Innovation and Development*, 0(0), 1–14. https://doi.org/10.1080/20421338.2020.1776061

Nzendjang Mbakouop, A., Nzoundja Fapi, C. B., Tchoffo Houdji, E., Tchakounté, H., & Innocentia Ankungha, A. (2025). Techno-economic Analysis of a Mixed Solar Dryer with Forced Convection: Profitability Study and Financial Feasibility. *Journal of Renewable Energy and Environment*.

Pangavhane, D. R., Sawhney, R. L., & Sarsavadia, P. N. (2002). Design, development and performance testing of a new natural convection solar dryer. *Energy*, 27(6), 579-590.

Prakash, O., & Kumar, A. (2013). Historical review and recent trends in solar drying systems. *International journal of green energy*, 10(7), 690-738.

Prakash, O., & Kumar, A. (Eds.). (2017). Solar drying technology: concept, design, testing, modeling, economics, and environment. Springer.

Radovanović, B., Mladenović, J., Radovanović, A., Pavlović, R., & Nikolić, V. (2015). Phenolic composition, antioxidant, antimicrobial and cytotoxic activites of Allium porrum L.(Serbia) extracts. *J Food Nutr Res*, 3(9), 564-9.

Ren, F., Perussello, C. A., Zhang, Z., Gaffney, M. T., Kerry, J. P., & Tiwari, B. K. (2018). Effect of agronomic practices and drying techniques on nutritional and quality parameters of onions (Allium cepa L.). *Drying Technology*, 36(4), 435-447.

Salhi, M., Chaatouf, D., Raillani, B., Amraqui, S., & Mezrhab, A. (2024). Experimental investigation and performance evaluation of an indirect solar dryer: Effect of drying trays. *Solar Energy*, 272, 112482.

Samtiya, M., Aluko, R. E., Dhewa, T., & Moreno-Rojas, J. M. (2021). Potential health benefits of plant food-derived bioactive components: An overview. Foods, 10(4), 839.

Sarkar, A., Hossain, M. W., Alam, M., Biswas, R., Roy, M., & Haque, M. I. (2023). Drying conditions and varietal impacts on physicochemical, antioxidant and functional properties of onion powder. *Journal of Agriculture and Food Research*, 12, 100578.

Sasongko, S. B., Hadiyanto, H., Djaeni, M., Perdanianti, A. M., & Utari, F. D. (2020). Effects of drying temperature and relative humidity on the quality of dried onion slice. Heliyon, 6.(7)

Savitha, S., Bhatkar, N., Chakraborty, S., & Thorat, B. N. (2021). Onion quercetin: As immune boosters, extraction, and effect of dehydration. *Food Bioscience*, 44, 101457.

Schiavone, D. F., Teixeira, A. A., Bucklin, R. A., & Sargent, S. A. (2013). Design and performance evaluation of a solar convection dryer for drying tropical fruit. *Applied Engineering in Agriculture*, 29(3), 391–401. https://doi.org/10.13031/aea.29.9896

Sharma, M., Atheaya, D., & Kumar, A. (2024). Optimizing hybrid household indirect solar dryer with sinusoidal corrugated Collector: CFD simulations and thermal performance analysis. *Solar Energy*, 279, 112817.

Shukir, S. S. (2021). Solar Energy Batteries-A Critical Review. *Journal of Instrumentation and Innovation Sciences*, 6(3), 25–30. www.matjournals.com

Siddiq, M., Roidoung, S., Sogi, D. S., & Dolan, K. D. (2013). Total phenolics, antioxidant properties and quality of fresh-cut onions (Allium cepa L.) treated with mild-heat. *Food chemistry*, 136(2), 803-806.

Singh, S., Gill, R. S., Hans, V. S., & Singh, M. (2021). A novel active-mode indirect solar dryer for agricultural products: Experimental evaluation and economic feasibility. *Energy*, 222, 119956.

Suraparaju, S. K., Elangovan, E., Muthuvairavan, G., Samykano, M., Elumalai, P. V., Natarajan, S. K., ... & Sivalingam, K. M. (2024). Assessing thermal and economic performance of solar dryers in sustainable strategies for bottle gourd and tomato preservation. Scientific Reports, 14(1), 27755.

Tedesco, F. C., Bühler, A. J., & Wortmann, S. (2019). Design, construction, and analysis of a passive indirect solar dryer with chimney. *Journal of Solar Energy Engineering*, 141(3), 031015.

Tiris, C., Tiris, M., & Dincer, I. (1995). Investigation of the thermal efficiencies of a solar dryer. *Energy Conversion and Management*, 36(3), 205–212. https://doi.org/10.1016/0196-8904(94)00051-Z

Wang, Y., Duan, X., Ren, G., & Liu, Y. (2018). Comparative study on the flavonoids extraction rate and antioxidant activity of onions treated by three different drying methods. *Drying Technology*, 37(2), 245–252. https://doi.org/10.1080/07373937.2018.1482907

Yaldiz, O., Ertekin, C., & Uzun, H. I. (2001). Mathematical modeling of thin layer solar drying of sultana grapes. *Energy*, 26(5), 457-465.

Yazici, M., & Kose, R. (2024). Energy, exergy and economic investigation of novel hybrid dryer, indirect solar dryer and traditional shade drying. *Thermal Science and Engineering Progress*, 49, 102502.

Zachariah, R., Maatallah, T., & Modi, A. (2021). Environmental and economic analysis of a photovoltaic assisted mixed mode solar dryer with thermal energy storage and exhaust air recirculation. *International Journal of Energy Research*, 45(2), 1879-1891.

Zaredar, A., Effatnejad, R., & Behnam, B. (2018). Construction of an indirect solar dryer with a photovoltaic system and optimised speed control. *IET Renewable Power Generation*, 12(15), 1807-1812.